MOLECULAR AND CELLULAR BIOLOGY, Feb. 2010, p. 985–994 Vol. 30, No. 4
0270-7306/10/$12.00 doi:10.1128/MCB.00909-09

The Ubiquitin Ligase Hul5 Promotes Proteasomal Processivity▽

Sharon Aviram and Daniel Kornitzer*

Department of Molecular Microbiology, B. Rappaport Faculty of Medicine, Technion-IIT and the Rappaport Institute for Research in the Medical Sciences, Haifa 31096, Israel

Received 13 July 2009/Returned for modification 19 October 2009/Accepted 7 December 2009

The 26S proteasome is a large cytoplasmic protease that degrades polyubiquitinated proteins to short peptides in a processive manner. The proteasome 19S regulatory subcomplex tethers the target protein via its polyubiquitin adduct and unfolds the target polypeptide, which is then threaded into the proteolytic site-containing 20S subcomplex. Hul5 is a 19S subcomplex-associated ubiquitin ligase that elongates ubiquitin chains on proteasome-bound substrates. We isolated *hul5*Δ as a mutation with which fusions of an unstable cyclin to stable reporter proteins accumulate as partially processed products. These products appear transiently in the wild type but are strongly stabilized in 19S ATPase mutants and in the *hul5*Δ mutant, supporting a role for the ATPase subunits in the unfolding of proteasome substrates before insertion into the catalytic cavity and suggesting a role for Hul5 in the processive degradation of proteins that are stalled on the proteasome.

Selective degradation of cellular short-lived or damaged proteins occurs via the ubiquitin-proteasome system (UPS). Substrates of the UPS are covalently conjugated to the polypeptide ubiquitin via a cascade of enzymatic reactions mediated by a ubiquitin-activating enzyme, ubiquitin-conjugating enzymes, and ubiquitin ligases (16). The product of this reaction cascade is a chain of ubiquitin adducts, typically based on an isopeptide bond between the ε-amino group of a lysine residue of the substrate and the C-terminal carboxyl group of ubiquitin and with subsequent ubiquitin molecules similarly bound to an internal lysine of the preceding ubiquitin adduct. Polyubiquitinated substrates are subsequently recognized and degraded by the 26S proteasome, a large multicatalytic proteinase consisting of a catalytic barrel-shaped 20S subcomplex and two regulatory 19S subcomplexes at either end. The 20S subcomplex carries three distinct proteolytic activities—a chymotrypsin, trypsin, and caspase-like activity—carried by three different protein subunits (15, 22, 33, 48). Access to the catalytic sites, which are located inside the lumen of the hollow 20S barrel, require passage through two narrow openings at either end of the barrel (12). This access is controlled by the 19S subcomplexes, the roles of which include binding polyubiquitinated proteins, unfolding the target polypeptide via a chaperone-like activity in order to allow it to be threaded into the 20S lumen, and hydrolyzing the polyubiquitin isopeptide bonds in order to recycle the ubiquitin (reviewed in references 6, 36, and 42). By analogy with eubacterial ATP-requiring proteases (29, 41) and archaebacterial proteasomes (44, 50), unfolding of the substrate protein by the 26S proteasome is thought to depend on the activity of a ring of six AAA-type ATPases located at the base of the 19S subcomplex, adjacent to the aperture of the 20S catalytic subcomplex of the proteasome (10).

Whereas most proteasome substrates are processively degraded to completion, some substrates, such as the NF-κB precursor p105, its *Drosophila melanogaster* homolog Ci, and the yeast transcription factors Spt23 and Mga2, exhibit partial processing, i.e., degradation of part of the polypeptide and release of another part (18, 35, 45). This is thought to result from a combination of a stably folded domain preceded, in the direction of polypeptide degradation, by a simple sequence repeat which may inhibit effective transfer of the polypeptide into the proteasome catalytic cavity (34, 37, 45).

Several proteasome-associated proteins have been found in yeast, including the deubiquitinating enzyme Ubp6 and the HECT-type ubiquitin ligase Hul5 (28, 47). KIAA10, the apparent mammalian homolog of Hul5, is also associated with the proteasome (3, 28, 49). Ubp6 constitutes one of at least two proteasome-associated deubiquitinating activities that participate in the recycling of the ubiquitin moieties of proteins targeted to the proteasome (13, 28, 46), and it is also involved in the trimming of the ubiquitin chains of substrates bound to the proteasome (3). On purified proteasomes, the latter activity is opposed by Hul5 (3). Although some UPS substrates have been found to be stabilized in the absence of Hul5, the mechanistic role of this ubiquitin ligase within the UPS remains unclear.

Pcl5 is a yeast cyclin-like protein that is rapidly degraded via two distinct degradation signals, an N-terminal phosphorylation-dependent signal and a C-terminal signal that requires a free carboxy-terminal end (1). Fusion of Pcl5 C-terminally to the normally stable enzyme Ura3 causes destabilization of the fusion construct (1). We used the instability of Ura3-Pcl5 to screen for yeast mutants that stabilize Pcl5. Here we describe the isolation of *hul5*Δ as a mutant that, rather than inhibiting turnover of Ura3-Pcl5, causes the fusion protein to be partially processed by the proteasome. Analysis of the kinetics of degradation or processing of various Pcl5 fusion proteins in different mutant strains indicates that ubiquitination by Hul5 is required, together with 19S ATPase activities, for full degradation of specific substrates.

* Corresponding author. Mailing address: Technion-IIT, Department of Molecular Microbiology, B. Rappaport Faculty of Medicine, 2 Efron St., Haifa 31096, Israel. Phone: 972-4-829 5258. Fax: 972-4-829 5254. E-mail: danielk@tx.technion.ac.il.

▽ Published ahead of print on 14 December 2009.

MATERIALS AND METHODS

S. cerevisiae* strains and growth conditions.** The following *S. cerevisiae* background strains were utilized: W303 (R. Rothstein), BY4741 (EUROSCARF), and sub62 (D. Finley). KY775 is W303 *pdr5*Δ::*hisG erg6*Δ::*hisG*. The *hul5*Δ::Kan^r and *ubp6*Δ::Kan^r alleles were obtained from EUROSCARF and combined by mating to generate the double mutant (KY1226: *MATa** *ura3 leu2 lys2 his3 ubp6*Δ::Kan^r *hul5*Δ::Kan^r). The *hul5*Δ::Kan^r allele was transferred by transformation of a PCR product of the *hul5*Δ::Kan^r genomic region into sub62 to generate KY1302 (*MAT***a** *ura3 leu2 lys2 his3 trp1 gal hul5*Δ::Kan^r), into sub62 *rpt2*^{RF} (40) to generate KY1303, and into KY775 to generate KY1270. The *crl3-2* strain used, KY774, was generated by backcrossing the original mutant (31) into W303 twice.

The strains were grown in standard yeast extract-peptone-dextrose (YPD) (1% yeast extract, 2% peptone, 2% dextrose) and complete yeast nitrogen base media (YNB) (1.5 g/liter yeast nitrogen base, 5 g/liter ammonium sulfate, 2% dextrose or galactose, 0.1 g/liter of each amino acid, uracil, and adenine, with the appropriate amino acids removed as required for plasmid selection).

Plasmid constructions. *PCL5* was cloned as a BamHI-XhoI PCR fragment in pOC9 (9) to generate KB1169 (CEN *TRP1 CUP1p-URA3*-HA-*PCL5*). The SacI-XhoI fragments of KB1169 and pOC9 were cloned into pRS313 to generate KB1432 (CEN *HIS3 CUP1p-URA3*-HA-*PCL5*) and KB1433 (CEN *HIS3 CUP1p-URA3*-HA). KB1908 to -1910 are identical to KB1432 except that fragments corresponding to *PCL5* codons 1 to 46, 1 to 53, and 1 to 65, respectively, were cloned instead of full-length *PCL5*. KB1943 (CEN *HIS3 MET25p*-GFP-*PCL5*), KB1951 (id. but with *PCL5* codons 40 to 229), and KB1952 (id. but with *PCL5* codons 71 to 229) consist of the *PCL5* sequences cloned as BamHI-XhoI PCR fragments into pUG34 (a gift of Johannes Hegemann). KB1954 and KB1955 consist of *HUL5* and *HUL5* C878A cloned as PstI-SacI fragments from plasmids pJH85 and pJH85 (3) into pRS315 (CEN *LEU2*). KB2012 contains the *GCN4* fragment extending between codons 62 and 202 from plasmid KB893 (32) fused to the *PCL5* open reading frame, under the *CUP1p* promoter on a *CEN TRP1* vector. *CUP1p*-Myc-*UBI* and *CUP1p-UBI* are described in reference 5.

Materials. MG132 (CbzLLLal) (27, 39) was obtained from Calbiochem. [^{35}S]methionine-cysteine (Easytag Express) was from Perkin-Elmer. Antibodies used were HA.11 (Covance, Princeton, NJ) anti-green fluorescent protein (GFP) polyclonal antibody (Invitrogen), polyclonal anti-Pcl5 (43), and polyclonal anti-Gcn4 (32). Protein A-Sepharose was from GE-Health Care.

Protein degradation analysis. Pulse-chase protein degradation analysis was done as described previously (25). Briefly, cells (10 ml) were grown in synthetic dropout medium to an optical density at 600 nm (OD_{600}) of 0.7 to 1.0, induced for 20 min with 0.2 mM $CuSO_4$ or by growing for several hours in methionine-depleted medium, spun down, and washed once in YNB medium supplemented with the essential amino acids only, resuspended in 0.3 ml of the same medium containing [^{35}S]methionine-cysteine (Easytag Express; Perkin-Elmer), and incubated for 5 min at 30°C. Cells were then spun down and resuspended in 2.5 ml synthetic complete (SC) medium containing 10 mM (each) methionine and cysteine. At the indicated times, an aliquot was removed, treated with NaOH (0.25 M) and β-mercaptoethanol (1%), incubated 10 min on ice, and then precipitated with 7% trichloroacetic acid (TCA). The protein pellet was washed with acetone and resolubilized in 2.5% SDS, and the Ura3-hemagglutinin (HA)-Pcl5, GFP-Pcl5, and Gcn4(62–202)-Pcl5 proteins were immunoprecipitated using the HA.11 antibody (Covance, Princeton, NJ), an anti-GFP polyclonal antibody (Invitrogen), or a polyclonal anti-Gcn4 antibody (32). The immunoprecipitates were analyzed by SDS-PAGE, and quantitation was carried out using a Fuji Bas phosphorimager plate. For quantitation of the Ura3-Pcl5 and GF-Pcl5 processing products, the radioactivity of the processed protein band was compared to that of the full-length protein band at time zero (t_0). However, to account for the fact that the processed band contains fewer labeled residues (methionine and cysteine), the processed-band percentages were adjusted accordingly: the processed Ura3-Pcl5 band intensity was multiplied by 20/11 (number of Met-Cys in full-length versus processed Ura3-Pcl5) and the GFP-Pcl5 processed-band intensity was multiplied by 2 (18 Met-Cys in GFP-Pcl5 versus 9 in the processed product).

Alternatively, protein stability was assayed by following the levels of specific proteins by use of Western blotting after arrest of protein synthesis. Synthesis arrest was achieved by adding the protein synthesis inhibitor cycloheximide (20 μg/ml) to the medium. Equal amounts of culture were spun down, incubated on ice for 10 min with NaOH (0.25 M) and β-mercaptoethanol (1%), and precipitated with 7% TCA. The protein pellet was washed with acetone, resolubilized in protein loading buffer, subjected to SDS-PAGE, and reacted with the HA.11 antibody, with polyclonal anti-GFP, or with polyclonal anti-Pcl5 (43), as required.

Identification of Ura3-Pcl5 processing product by mass spectroscopy. *hul5*Δ cells (KY985) carrying the *CUP1p-URA3-HA-PCL5* plasmid (KB1432) or a vector plasmid were grown at 30°C in 50 ml synthetic dropout medium to an OD_{600} of 2, and then $CuSO_4$ was added to 0.1 mM and the culture was incubated for a further 30 min. The cells were pelleted, washed twice, resuspended in 3 ml ice-cold immunoprecipitation (IP) buffer with antiproteases (25), and mechanically disrupted with a bead beater. The extracts were centrifuged at 13,000 × *g* for 15 min, and then the supernatant was saved and mixed with about 60 μl (about 12 μg) of HA.11 antibody (Covance). After 90 min of incubation at 4°C, 20 μl of protein A beads (Pharmacia) were added and the extracts were incubated for another 90 min at 4°C while tumbling. The beads were washed five times and then resuspended in gel loading buffer, and the immunoprecipitate was subjected to SDS-PAGE. On the Coomassie-stained gel, an ~35-kDa band was clearly visible in the Ura3-Pcl5 lane and absent in the vector lane. This band was cut out of the gel, and the gel slice was treated as follows. The proteins in the gel were reduced with 3 mM dithiothreitol (DTT) (60°C for 30 min) and modified with 120 mM iodoacetamide in 10 mM ammonium bicarbonate (room temperature for 30 min). The gel pieces were dehydrated with acetonitrile and rehydrated with 10% acetonitrile in 10 mM ammonium bicarbonate containing trypsin (modified trypsin [Promega] at a 1:20 enzyme-to-substrate ratio). The gel pieces were incubated overnight at 37°C, and the resulting peptides were recovered and resolved by reverse-phase chromatography on 0.1- by 200-mm fused silica capillaries (100-μm inside diameter; J&W) packed with Everest reversed-phase material (Grace Vydac, California). The peptides were eluted with linear 50-min gradients of 5 to 95% of acetonitrile with 0.1% formic acid in water at flow rates of 0.4 μl/min. Mass spectrometry (MS) was carried out by an ion trap mass spectrometer (LCQ-DecaXP; Finnigan, San Jose, CA) in a positive mode using a repetitively full MS scan followed by collision-induces dissociation (CID) of the 3 most dominant ions selected from the first MS scan.

The mass spectrometry data were clustered and analyzed using the Sequest software program (J. Eng and J. Yates, University of Washington, and Finnigan, San Jose, CA), searching against the yeast sections of the NR-NCBI database and against the specific sequence of the protein. Significant peptide identification had Sequest XCorr values of 1.5 for singly charged peptides, 2.5 for doubly charged peptides, and 3 for triply charged peptides.

IP/Western blotting for detection of Ura3-Pcl5 ubiquitination. Wild-type (wt) and *hul5*Δ mutant cells carrying the indicated plasmids (see the legend to Fig. 4) were grown for 4 h in SC medium supplemented with 0.2 mM $CuSO_4$, harvested, and mechanically disrupted with a bead beater in lysis buffer (10 mM HEPES [pH 7.5], 2.5 mM SDS, 5 mM EDTA, 1:500 of a cocktail of leupeptin, chymostatin, and pepstatin [10 mg/ml in dimethyl sulfoxide, 1 mM phenylmethylsulfonyl fluoride, and 5 mM *N*-ethylmaleimide [NEM]). Equal amounts of protein extract were diluted at least 10-fold in IP buffer (50 mM HEPES [pH 7.5], 1% Triton X-100, and EDTA, antiproteases, and NEM as for lysis buffer) and incubated with tumbling at 4°C with HA.11 Sepharose beads (Covance) for 3 h. The beads were washed four times with IP buffer supplemented with 0.1% SDS and then eluted by boiling in gel loading buffer. The protein extract was analyzed by SDS-PAGE and Western blotting, using the 9E10 anti-Myc antibody to detect Myc-ubiquitin.

Growth tests. Yeast strains were precultured to the same optical densities (OD_{600} = 1) and spotted onto appropriate YNB-based media, supplemented as indicated. Fivefold dilutions, starting with 5 × 10^3 cells per 5 μl, were spotted onto the plates, incubated at 30°C for various periods, and photographed under white light.

RESULTS

A 36-kDa degradation product of Ura3-Pcl5 is generated in the *hul5*Δ mutant. In order to identify mutants that would stabilize the Ura3-Pcl5 fusion, we used a *CUP1p*::*URA3-HA-PCL5* plasmid construct previously shown to be unable to confer uracil prototrophy due to rapid turnover of Ura3-Pcl5 (1). We screened the EUROSCARF yeast deletion collection for growth on uracil-depleted plates, using two methods: by transforming the *CUP1p*::*URA3*-HA-*PCL5* plasmid into a pooled strain collection and selecting for uracil prototrophy and by transforming some 120 individual strains representing deletion mutants in the UPS with the plasmid, followed by testing of the transformants for growth on uracil-depleted plates. The only mutant that was consistently recovered from the whole deletion collection pool was

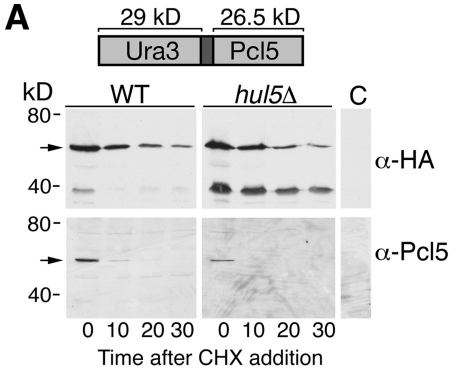

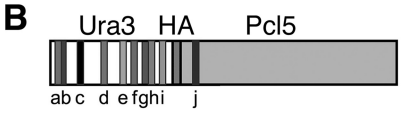

Peptide	Sequence	Protein identification
a	K.QTNLCASLDVR.T	Ura3
b	K.ELLELVEALGPK.I	Ura3
c	K.YNFLLFEDR.K	Ura3
d	R.IAEWADITNAHGVVGPGIVSGLK.Q	Ura3
e	R.GLLMLAELSCK.G	Ura3
f	K.SDKDFVIGFIAQR.D	Ura3
g	R.DEGYDWLIMTPGVGLDDKGDALGQQYR.T	Ura3
h	R.TVDDVVSTGSDIIIVGR.G	Ura3
i	K.AGWEAYLR.R	Ura3
j	K.EFNTVVK.S	Pcl5

FIG. 1. Expression of Ura3-Pcl5 in *hul5*Δ mutant cells generates a 36-kDa Ura3-containing species. (A) The schematic drawing of the fusion protein indicates the positions of the Ura3 and Pcl5 moieties, with the intervening HA tag indicated in dark gray. Cells were induced with $CuSO_4$ and treated with cycloheximide (CHX) as detailed in Materials and Methods. Upper panel: detection of the Ura3-HA-Pcl5 fusion with the HA.11 antibody (α-HA). Lower panel: detection of the same membrane with an anti-Pcl5 antiserum (α-Pcl5). (B) Mass-spectrometry analysis of the 36-kDa species after digestion with trypsin (see Materials and Methods for details). The origins of the identified peptides are indicated, and their distribution on the Ura3-Pcl5 sequence is depicted schematically.

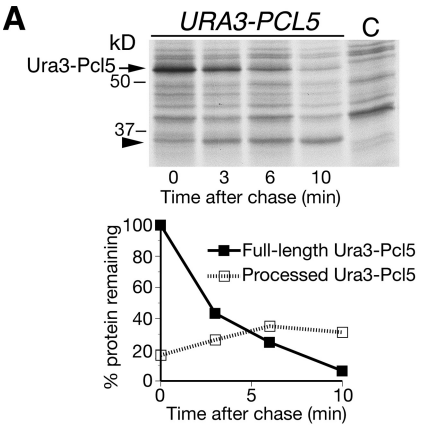

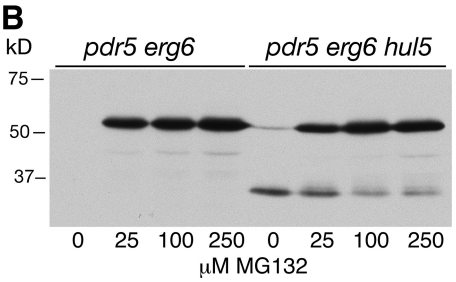

FIG. 2. The Ura3-Pcl5 processing product is a consequence of proteasome activity. (A) Pulse-chase analysis of Ura3-Pcl5 degradation in *hul5*Δ mutant cells. Cells carrying plasmid KB1432 expressing the Ura3-Pcl5 fusion protein were labeled for 2 min and chased with cold methionine. C, cells carrying a vector plasmid. The 36-kDa processing product is indicated with an arrowhead. The graph depicts the quantitation of the experiment shown; the percentage of the processing product is indicated relative to the full-length protein at t_0 of the chase, corrected for the smaller number of methionines and cysteines (the residues labeled with ^{35}S) in the processing product, namely, 11, versus 20 in the full-length Ura3-Pcl5 fusion protein. (B) Accumulation of Ura3-Pcl5 and its processing product upon proteasome inhibition. Strains KY775 (*pdr5 erg6*) and KY1270 (*pdr5 erg6 hul5*) carrying plasmid KY1169 were incubated for 20 min with 0.2 mM CuSO4 (Ura3-Pcl5 induction) and with the indicated amounts of the proteasome inhibitor MG132 before protein extraction.

the *hul5*Δ mutant. Furthermore, among the 120 individual UPS mutants, the *hul5*Δ mutant was again the mutant that exhibited the most robust growth on uracil-depleted plates.

We tested directly degradation of full-length Pcl5 expressed under the *CUP1* promoter in the *hul5*Δ strain but saw no difference in half-life in the mutants versus the wild-type strain (data not shown). We therefore went back to the Ura3-Pcl5 fusion protein that served as a reporter in the growth screen and checked its steady-state levels and stability after translation inhibition with cycloheximide in the wt versus the *hul5*Δ strain (Fig. 1). The steady-state levels and stability of the Ura3-Pcl5 fusion protein (57 kDa; indicated by an arrow in Fig. 1) were unchanged for the various mutant strains versus results for the wild type. However, in the *hul5*Δ strain, a faster-migrating protein band of about 36 kDa accumulated. A similar, but weaker, protein band was transiently visible in the wild-type strain before cycloheximide addition but disappeared rapidly afterwards (Fig. 1A, upper panel). An anti-Pcl5 polyclonal antibody reacted only with the upper band (Fig. 1A, lower panel). Furthermore, since the 36-kDa protein band was visualized with the anti-HA antibody and since the HA epitope tag is located between the Ura3 (29 kDa) and Pcl5 (26.5 kDa) sequences in this construct, we surmised, based on the uracil prototrophy of the *hul5*Δ mutant, that this band represents a partial degradation product, containing Ura3 and the N-terminal fragment of Pcl5. This was confirmed by MS analysis of tryptic peptides of the 36-kDa protein band, which identified nine peptides along the length of the Ura3 sequence and a single peptide corresponding to the Pcl5 sequence between positions 12 and 21 (Fig. 1B).

The 36-kDa protein band could represent a degradation product of the full-length Ura3-Pcl5 fusion; alternatively, it could be a consequence of incomplete synthesis of the fusion protein. To distinguish between these possibilities, we performed a pulse-chase analysis of *hul5*Δ mutant cells expressing the fusion protein. As shown in Fig. 2A, after a short pulse-labeling period, the 36-kDa band increased in intensity during the 10 min of the chase, concomitant with the disappearance of the full-length protein, suggesting a precursor-product relationship and supporting the assumption that the 36-kDa protein band represents a degradation product of the full-length Ura3-Pcl5 fusion. Quantitation of the relative increase of the processing product versus the decrease of the full-length prod-

uct in the first 6 min of the chase indicates that about 25% of the full-length product was processed to the shorter product whereas the remainder was degraded to completion.

The 36-kDa degradation product is generated by incomplete proteasomal degradation. The rapid disappearance of the 36-kDa band in the wild type and its stabilization in the *hul5*Δ mutant could have been due to incomplete degradation of the Ura3-Pcl5 fusion by the proteasome. Alternatively, this band could represent a proteolytic cleavage product, unrelated to proteasome activity, that is normally very rapidly degraded via a pathway involving the Hul5 ubiquitin ligase. If the latter were true, then chemical inhibition of the catalytic activity of the proteasome should lead to the same accumulation of the 36-kDa band as seen in the *hul5*Δ mutant. To test this, we exposed drug-permeable *pdr5*Δ *erg6*Δ strains, either wild type or deleted for *HUL5*, to increasing concentrations of the proteasomal inhibitor MG132 (CbzLLLal) (27, 39]) and at the same time induced Ura3-Pcl5 production from the *CUP1p*::*URA3-HA-PCL5* plasmid. The full-length Ura3-Pcl5 protein accumulated greatly in the presence of the drug, both in the wild-type strain and the *hul5*Δ strain, confirming that Ura3-Pcl5 is normally degraded via the proteasome (Fig. 2B). In the wild-type strain, however, the 36-kDa band was undetectable even in the presence of MG132. Furthermore, in the *hul5*Δ mutant, appearance of the 36-kDa processing product decreased with increasing amounts of MG132 (Fig. 2B). These data suggest that appearance of the 36-kDa band does require proteasome activity, rather than representing a proteasome-independent cleavage event, and thus support the first possibility, i.e., that it represents incomplete degradation of Ura3-Pcl5 by the proteasome.

Hul5 was identified as a ubiquitin ligase associated with the proteasome (3, 28). Thus, one possibility is that the role of Hul5 is to promote the processivity of Ura3-Pcl5 degradation on the proteasome. Alternatively, unrelated to its function on the proteasome, Hul5 could be required in a cytoplasmic ubiquitination and degradation pathway of the 36-kDa processing product that is normally released by the proteasome. To address the latter possibility, it was necessary to determine whether the 36-kDa product, when synthesized independently, is subject to Hul5-dependent degradation. The site of final proteasomal cleavage of Ura3-Pcl5 in *hul5*Δ cells was determined in the following way. In the first stage, potential proteasome cleavage sites in the Pcl5 region corresponding to the 36-kDa fragment (around position 50 in the Pcl5 sequence) were predicted using the PAProC algorithm (26). The predicted proteasomal cleavage sites closest to position 50 were located after positions 46, 47, and 53. In a second stage, Ura3-Pcl5 fusion constructs extending to positions 46, 53, and 65 of Pcl5 were compared by SDS-PAGE to the Ura3-Pcl5 processing product that appears in the *hul5*Δ mutant. As can be seen in Fig. 3A, the Ura3-Pcl5 proteasomal processing product migrates identically to the Ura3-Pcl5(1–53) construct and is easily distinguished from the 1–46 and 1–65 constructs. We estimate that differences of more than 1 residue in the length of the processing product would have been detectable, i.e., the 36-kDa processing product consists of Ura3-Pcl5(1–53+/− 1). We then asked whether the Ura3-Pcl5(1–53) protein is degraded via Hul5. However, this protein is stable (Fig. 3B), which is inconsistent with it being degraded via a proteasome-independent function of Hul5 but consistent with a role for Hul5 in the processivity of Ura3-Pcl5 degradation by the 26S proteasome.

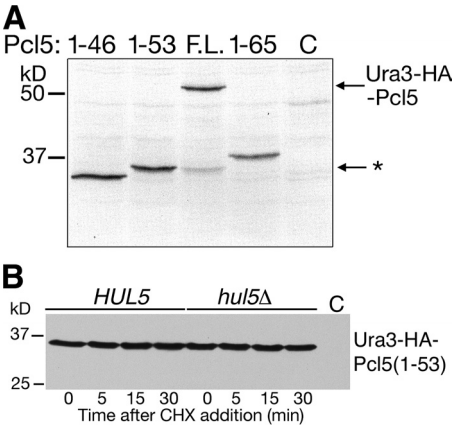

FIG. 3. The Ura3-Pcl5 processing product is not inherently unstable. (A) Characterization of the Ura3-Pcl5 processing product size. Wild-type cells expressing Ura3 fused to various fragments of Pcl5 from plasmids KB1908 (1–46), KB1909 (1–53), KB1910 (1–65), or *hul5*Δ mutant cells expressing full-length Ura3-Pcl5 (F.L.) were pulse-labeled for 10 min and then subjected to immunoprecipitation and SDS-PAGE. (B) Ura3-Pcl5(1–53) expressed from KB1909 in wild-type and *hul5*Δ cells was subjected to stability analysis as for Fig. 1A.

Catalytic activity of Hul5 is required for processive Ura3-Pcl5 degradation. Hul5 extends ubiquitin chains on proteasome-tethered substrates *in vitro*, an activity that requires an essential cysteine in the HECT domain of the protein (3, 28). We therefore tested whether ubiquitin ligase activity of Hul5 is required for its effect on the processivity of Ura3-Pcl5 degradation. We first tested whether Hul5-dependent polyubiquitination of Ura3-Pcl5 could be detected *in vivo*. Ura3-Pcl5 isolated from cells expressing Myc-tagged ubiquitin was immunoprecipitated and reacted with the anti-Myc antibody. A high-molecular-weight smear, which was Ura3-Pcl5 and Myc-ubiquitin dependent, was clearly visible for the *HUL5* strain but almost totally absent for the *hul5*Δ strain (Fig. 4A). This is consistent with polyubiquitination of Ura3-Pcl5 being dependent upon Hul5. Next, we tested whether the catalytic activity of Hul5 was involved in the growth phenotype of cells expressing Ura3-Pcl5. *hul5*Δ cells expressing Ura3-Pcl5 were transformed with plasmids containing wild-type *HUL5* or the *hul5* C878A mutant, which is catalytically inactive *in vitro* (3, 28). Whereas wild-type *HUL5* was able to suppress the uracil prototrophy of the *hul5*Δ strain expressing Ura3-Pcl5, the *hul5* C878A mutant was unable to do so (Fig. 4B). Finally, we tested the effect of the *hul5* C878A mutant directly on the processing of Ura3-Pcl5 by the proteasome. Complementation of the Ura3-Pcl5 processing defect of the *hul5*Δ mutation indicated that compared to wild-type *HUL5*, the *hul5* C878A mutant is almost totally inactive for processive Ura3-Pcl5 degradation (Fig. 4C). Taken together, the data shown in Fig. 4 indicate that Hul5-mediated polyubiquitination is essential for processive degradation of Ura3-Pcl5 by the proteasome.

Genetic interaction between *hul5*Δ and *ubp6*Δ in Ura3-Pcl5 processing. Hul5 was identified as one of several proteasome-associated proteins. Another proteasome-associated protein is Ubp6, a ubiquitin hydrolase (28, 47). Hul5 and Ubp6 were

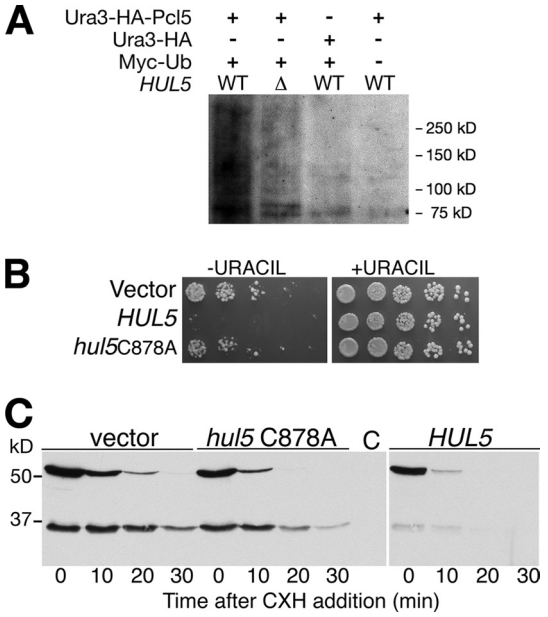

FIG. 4. Ura3-Pcl5 is ubiquitinated by Hul5. (A) sub62 cells, either wild type or *hul5*Δ mutant, transformed with either KB1432 (Ura3-HA-Pcl5) or KB1432 (Ura3-HA) and either *CUP1p*-Myc-*UBI* or *CUP1p-UBI* (5) were induced for 4 h with 0.2 mM $CuSO_4$. In a first stage, Ura3-Pcl5 was immunoprecipitated with an anti-HA antibody, and then the precipitate was solubilized in gel loading buffer and analyzed by SDS-PAGE/Western blotting for the presence of Myc-reactive proteins. (B) Strain KY1302 (sub62 *hul5*Δ) transformed with either KB1954 (*HUL5*), KB1955 (*hul5* C878A), or vector (pRS315) and 5-fold dilutions of the resulting strains were spotted on synthetic complete medium without leucine and with or without uracil and incubated for 2 days (+uracil) or 3 days (−uracil). (C) Strain KY1302 was transformed with KB1169 (Ura3-Pcl5) and with either KB1954 (*HUL5*), KB1955 (*hul5* C878A), or vector (pRS315). Ura3-Pcl5 degradation was followed by cycloheximide translation inhibition as for Fig. 1A.

found to have opposing effects on polyubiquitination of proteasome-associated proteins *in vitro* (3). We therefore tested whether Hul5 and Ubp6 similarly have opposing effects on Ura3-Pcl5 degradation. The single and double mutant strains were analyzed for growth in the absence of uracil and for Ura3-Pcl5 degradation. The uracil prototrophy of the *hul5*Δ strain was not reverted by the additional *ubp6*Δ deletion (Fig. 5A); furthermore, the processing defect of the *hul5*Δ strain was not abolished by the additional deletion of *UBP6* (Fig. 5B). Interestingly, the *ubp6*Δ deletion itself showed some minor accumulation of the processed product (Fig. 5B). In accordance with this minor processing defect, a limited extent of growth was detectable with the *ubp6*Δ strain compared to that with the wild-type strain after more-extended incubation on uracil-depleted plates (Fig. 5A). Ura3-Pcl5 processing and degradation in these mutants were then quantitatively assessed by [^{35}S]methionine pulse-chase analysis (Fig. 5C). The transient appearance of processing product in the *ubp6*Δ mutant is detectable here as well (left panel); the processing product that is generated is rapidly degraded. When comparing the *hul5*Δ strain to the double *ubp6*Δ *hul5*Δ deletion strain (right panel), no difference in degradation of the full-length product was detected, but a decrease in accumulation of the processed product was detected in the double mutant—from 34% ± 7% in the *hul5*Δ strain to 21% ± 3.5% in the double *ubp6*Δ *hul5*Δ deletion strain. These data suggest that Ubp6 in the wild-type background promotes Ura3-Pcl5 processing; to the extent that Ura3-Pcl5 processing requires ubiquitination, the positive role of Ubp6 may reflect its role in maintaining ubiquitin homeostasis in the cell by sparing ubiquitin from degradation along with the UPS substrates (2, 14, 28). In the *hul5*Δ background, in contrast, deletion of *UBP6* somewhat mitigates the Ura3-Pcl5

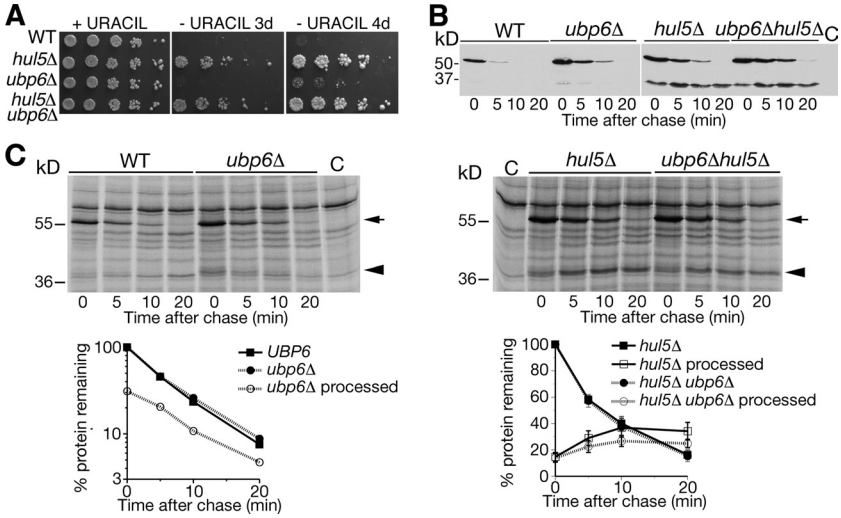

FIG. 5. Genetic interaction between *hul5*Δ and *ubp6*Δ in Ura3-Pcl5 processing. (A) Uracil prototrophy in the *hul5*Δ, *ubp6*Δ, and double mutants. Fivefold dilutions of the indicated mutants carrying plasmid KB1432 were spotted on synthetic complete medium with or without uracil and incubated for 2 days (+uracil) or 3 or 4 days (−uracil), as indicated, at 30°C. (B) The same strains were analyzed for Ura3-Pcl5 processing by cycloheximide chase as in Fig. 1A. (C) To quantitate the relative effect of Hul5 and Ubp6 on Ura3-Pcl5 processing, the same strains were subjected to [^{35}S]methionine pulse-chase analysis as described in Materials and Methods, and the Ura3-Pcl5 full-length and processing products were detected with the anti-HA antibody. The arrows indicate the position of full-length Ura3-Pcl5, and the arrowheads indicate the position of the processed product. Quantitation of the protein bands is represented in the graphs. For the *hul5*Δ versus *ubp6*Δ *hul5*Δ experiment, the graph represents the average of results from four experiments; bars indicate standard deviations. Quantitation of the processing product was corrected for the smaller number of labeled residues as in Fig. 2A.

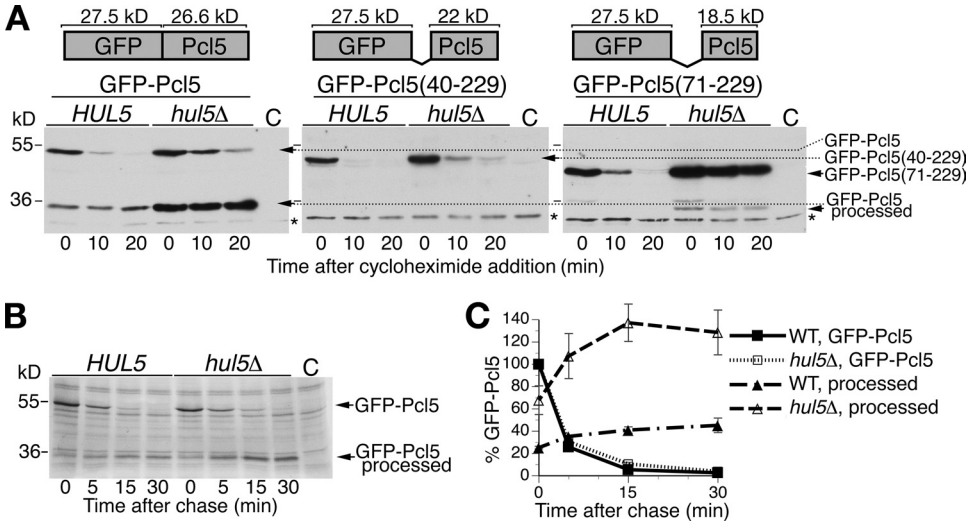

FIG. 6. Partial processing of GFP-Pcl5 fusions. (A) Cycloheximide chase of GFP-Pcl5, GFP-Pcl5(71–229), and GFP-Pcl5(71–229) expressed from plasmids KB1943, KB1951, and KB1952 in wild-type (sub62) versus *hul5*Δ (KY1302) cells. The asterisk indicates a nonspecific band. C, no-GFP control. (B) [^{35}S]methionine pulse-chase analysis of GFP-Pcl5 in wild-type versus *hul5*Δ cells. C, no-GFP control. (C) Quantitation of GFP-Pcl5 degradation versus processing (average of 2 experiments, included that shown in panel B). The percentage of the processing product is indicated relative to the full-length protein at t_0 of the chase, corrected for the smaller number of methionines and cysteines (the residues labeled with ^{35}S) in the processing product, namely, 9, versus 18 in the full-length GFP-Pcl5 fusion protein. Note that the processed band exceeds 100% in the *hul5*Δ mutant because the stable GFP band started accumulating during the pulse-labeling period.

processing defect; this may reflect the opposing effects of Ubp6 and Hul5 on ubiquitination of proteasome-bound proteins *in vitro* (3).

Partial processing of GFP-Pcl5. To better understand the role of Hul5 in Ura3-Pcl5 processing, we next sought to identify the reason for the failure of the cells to degrade this specific protein to completion. Targeting of Ura3-Pcl5 to the proteasome presumably occurs via the normally unstable Pcl5 moiety. The data shown above suggest that processive degradation of the fusion protein from its C terminus is transiently halted in the wild-type cells at position 53 of Pcl5. One possibility is that the stability of the Ura3 domain of the fusion protein prevents its unfolding, which is necessary for threading the polypeptide chain into the catalytic cavity of the 20S proteasome.

If the thermodynamic stability of Ura3 impedes processive degradation of the Ura3-Pcl5 fusion protein, then replacing Ura3 with green fluorescent protein (GFP), a protein shown in various contexts to be unusually hard to degrade processively (30, 51), may also inhibit full degradation of the fusion protein. Degradation of GFP-Pcl5 in both wild-type and *hul5*Δ cells was followed by cycloheximide chase (Fig. 6A, left panel). Whereas the full-length protein disappeared rapidly in both strains, albeit somewhat more slowly in the mutant strain, an ~33-kDa degradation product accumulated in both the wild-type and mutant cells but with a significantly higher accumulation visible in the *hul5*Δ mutant cells. To quantitate the extent of partial processing versus full degradation, a [^{35}S]methionine pulse-chase analysis of GFP-Pcl5 was carried out (Fig. 6B). Quantitation of GFP-Pcl5 degradation and processing indicated that in wild-type cells, of the 95% ± 2% of the protein degraded in the first 15 min of the chase, a small fraction of 15% ± 5% of the protein was processed to an ~33-kDa species rather than degraded. In the *hul5*Δ mutant, of the 90% ± 2% of the protein degraded in the first 15 min of the chase, 70% ± 5% of the protein was processed rather than degraded (Fig. 6C, average of 2 experiments). Thus, the presence of the stable GFP domain presents an impediment to processive degradation of the Pcl5 moiety of the fusion protein in wild-type cells but more so in the *hul5*Δ mutant cells.

Since 33 kDa is the expected size of the GFP-Pcl5 fusion extending to position 53 of Pcl5, it would appear that processive degradation of Pcl5 is inhibited at a similar location in the context of both Ura3 and GFP fusion proteins. In order to test the role of the N-terminal sequences of Pcl5 in the inhibition of processive degradation of GFP-Pcl5, we made deletion variants of Pcl5 in the context of the GFP-Pcl5 fusion protein. Degradation of GFP-Pcl5(40–229), which still includes the predicted processing site (position 53 of Pcl5), and GFP-Pcl5(71–229), lacking this site, was followed in both wild-type and *hul5*Δ cells by cycloheximide chase (Fig. 6A, middle and right panels). With the GFP-Pcl5(40–229) construct, no processing intermediate was detectable in either strain. With the GFP-Pcl5(71–229) construct, an ~34-kDa intermediate was transiently visible in both wild-type and *hul5*Δ mutant cells, but it did not accumulate, and a slightly smaller product was seen to accumulate in the *hul5*Δ mutant. These results suggest that, in addition to a stable protein domain, the accumulation of the degradation intermediates depends on the nature of the sequences near the processing site.

Processive degradation of Gcn4(62–202)-Pcl5. If in GFP-Pcl5, as in Ura3-Pcl5, processive degradation is impeded due to the thermodynamic stability of the GFP and Pcl5 moieties, then conversely, replacing Ura3 with a less stably folded protein domain should enable full degradation of the fusion protein. In our search for unstructured protein domains, we turned to activation domains of transcription factors, which are often relatively tolerant of deletions and point mutations. This

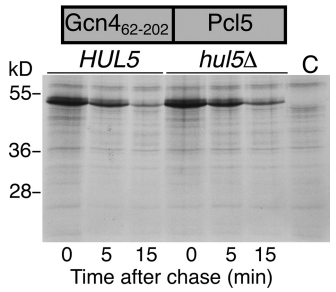

FIG. 7. Processive degradation of Gcn4(62–202)-Pcl5. Gcn4 T165A (62–202) was expressed from the *CUP1* promoter of plasmid KB2012 in wild-type (sub62) cells versus *hul5*Δ (KY1302) cells. Degradation of the fusion protein was followed by [^{35}S]methionine pulse-chase analysis. C, vector control.

is the case with Gcn4, which was shown to carry several short, partially redundant sequence elements that contribute to transcriptional activation (17, 20). Although there is little information regarding the structure of the Gcn4 activation domain, these observations are at least consistent with an absence of strong tertiary structure in this region of the protein. We therefore tested degradation of a fusion protein consisting of the Gcn4 region extending from position 62 to 202, encompassing part of the N-terminal activation domain and of the central acidic activation domain (17, 20), fused to full-length Pcl5. Since this region of Gcn4 also contains a degradation signal centered on Thr165 (32), we used a mutation in this critical threonine residue, T165A. Gcn4 T165A(62–202) fused to an epitope tag is stable and migrates aberrantly as an ~30-kDa polypeptide (32; our unpublished results). Degradation of Gcn4 T165A(62–202)-Pcl5, which migrates as an ~52-kDa protein, was followed using an anti-Gcn4 antibody. This fusion protein was rapidly degraded, both in the wild type and in the *hul5*Δ strain (Fig. 7). Strikingly, no degradation intermediates were detectable, even transiently, in either the wild-type or the *hul5*Δ background. This suggests that the nature of the domain fused to Pcl5 influences the processivity of degradation.

19S ATPase subunit mutants are defective in Ura3-Pcl5 degradation. Substrates need to be unfolded in order to be translocated into the 20S proteasome cavity. The unfolding activity is thought to depend mainly on the six AAA-type ATPases of the 19S subunit "base" subcomplex, which form a ring adjacent to the 20S aperture. If the incomplete degradation of Ura3-Pcl5 in the *hul5*Δ mutant and the transient appearance of the 36-kDa intermediate in the wild-type cells are due to a difficulty in unfolding of this protein by the 19S ATPases, then we might expect that mutant variants of these proteins would exhibit a phenotype similar to that of the *hul5*Δ mutant. We tested degradation of Ura3-Pcl5 in three ATPase mutants: a *crl3-2* mutant (= RPT6 [7]), a *cim5-1* mutant (= RPT1 [8]), and an *rpt2*^{RF} mutant (40). The last two showed clear accumulation of the 36-kDa processing product (data not shown), suggesting that processivity of Ura3-Pcl5 degradation is hampered by reduced ATPase activity and by deletion of *HUL5*. Since *rpt2*^{RF} is the best-characterized mutation, defective in the ATPase catalytic site of the protein (40), we chose this mutant to test the interaction between Hul5 and 19S ATPase activities. We tested the epistatic relationship of

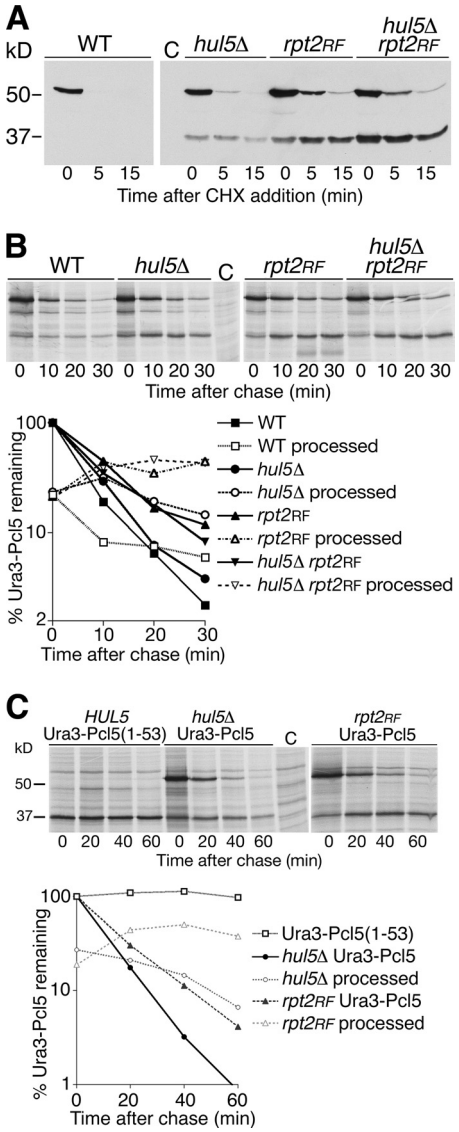

FIG. 8. Partial processing of Ura3-Pcl5 in the proteasomal ATPase mutant *rpt2*^{RF}. (A) Cycloheximide-chase analysis of Ura3-Pcl5 processing in the *hul5*Δ, *rpt2*^{R}F, and double mutants (strains KY1302, KY929, and KY1303, respectively). (B) Pulse-chase analysis of Ura3-Pcl5 using the same strains. (C) Pulse-chase analysis of Ura3-Pcl5 in KY929 and KY1302 versus Ura3-Pcl5(1–53) in wild-type cells. The two former strains were induced with 0.2 mM $CuSO_4$, whereas the latter strain was induced with 10 μM $CuSO_4$. Quantitation of the processing product in panels B and C was corrected for the smaller number of labeled residues as in Fig. 2A.

rpt2^{RF} and *hul5*Δ by comparing Ura3-Pcl5 degradation in single and double mutants by cycloheximide translation inhibition. Figure 8A shows that *rpt2*^{RF} is epistatic over *hul5*Δ: the *rpt2*^{RF} mutant shows the same Ura3-Pcl5 degradation and processing defect as the double mutant. Furthermore, comparison of the *rpt2*^{RF} and *hul5*Δ mutants indicated that the *rpt2*^{RF} mutant exhibits both a relative defect in degradation of full-length Ura3-Pcl5 and a more pronounced accumulation of the processing product. Quantitative examination of the kinetics of degradation by pulse-chase analysis confirmed that full-length

Ura3-Pcl5 is indeed degraded more slowly in the *rpt2*^{RF} mutant and indicated that whereas the Ura3-Pcl5(1–53) product was stable in the *rpt2*^{RF} mutant, in the *hul5*Δ mutant this product was degraded, with a half-life of about 20 min (Fig. 8B). We thus reexamined the kinetics of Ura3-Pcl5 degradation during a more extended chase period, in the *hul5*Δ strain versus the *rpt2*^{RF} strain, and compared it to the kinetics of degradation of Ura3-Pcl5(1–53) synthesized from the truncated *CUP1p-URA3-PCL5(1–53)* construct. To ascertain that the stability of the truncated Ura3-Pcl5(1–53) protein is not due to a higher level of expression, which might swamp its putative degradation system, we induced the *CUP1p-URA3-PCL5(1–53)* construct with a lower concentration of $CuSO_4$. The data in Fig. 8C indicate that the truncated Ura3-Pcl5(1–53) protein is completely stable in spite of being generated at only 2-fold-higher levels at most compared to the Ura3-Pcl5(1–53) processing product in the *hul5*Δ and *rpt2*^{RF} mutants. The fate of the processing product was different in the two mutants: in the *hul5*Δ mutant it was degraded with a half-life of about 20 min, whereas in the *rpt2*^{RF} mutant it appeared largely stable.

DISCUSSION

Hul5 was previously shown to be a proteasome-associated ubiquitin ligase which promotes proteasome activity *in vivo* and which is able to extend ubiquitin chains on proteasome-associated substrates *in vitro* (3, 28). Here we have shown that the *hul5*Δ mutant exhibits accumulation of a partial degradation product of the Ura3-Pcl5 fusion protein. This protein is the product of incomplete proteasomal degradation, as evidenced by the observation that a chemical inhibitor of the proteasome inhibits the generation of the Ura3-Pcl5 partial degradation product and that proteasomal 19S ATPase subunit mutants exhibit increased generation of this partial degradation product.

ATP-dependent proteases in general, and the 26S proteasome in particular, possess an impressive capacity for degrading folded proteins (24). Nonetheless, some proteins are refractory to complete degradation. By analogy with the few instances of naturally occurring partially processed proteasome substrates (18, 35, 45) and with degradation of some artificial hybrid substrates (21, 38), one can surmise that generation of the incomplete proteasomal degradation product of the Ura3-Pcl5 fusion protein is due to the confluence of two factors: (ii) a relatively strongly structured protein domain, in this case Ura3, and (ii) a sequence that impairs effective pulling of the polypeptide into the proteasomal catalytic cavity, in this case a sequence within the N-terminal region of Pcl5. Regarding the first factor, we find that the hard-to-unfold GFP protein (30), fused N-terminally to Pcl5, elicits incomplete processing even in the *HUL5* wild-type background, underscoring the significance of the domain structure in incomplete versus complete degradation by the proteasome. Conversely, replacement of Ura3 with a transcription activation domain, Gcn4(62–202), assumed to have low thermodynamic stability, did allow full degradation of the fusion protein. The importance of the second factor, a sequence in the Pcl5 region adjacent to the stable protein moiety, is revealed by the finding that deletions in the Pcl5 N-terminal region of the GFP-Pcl5 fusion protein either diminish or abrogate the production of a degradation intermediate. This specific sequence at the Pcl5 N terminus might be akin to the GA repeat sequence of EBNA1, which in certain contexts interferes with processive proteasomal degradation (19, 51), possibly because it prevents the ATPases from exerting sufficient traction on the polypeptide to unravel the adjacent protein domain. There are no apparent simple repeat sequences in the Pcl5 N-terminal domain, but sequences that interfere with polypeptide transfer into the proteasome are not necessarily readily recognizable (45).

Hul5's role could be to promote the processivity of the proteasome. Alternatively, given the rapid disappearance of the Ura3-Pcl5(1–53) processing product in the wild-type strain versus its slow turnover in the *hul5*Δ mutant, Hul5 could be required for degradation of this processing product independently of the proteasome. This would be analogous to a role recently suggested by Kohlmann et al. for Hul5 in degradation of the partial proteasome degradation product from an artificial endoplasmic reticulum (ER)-associated degradation (ERAD) substrate (23). However, several observations suggest that Hul5 acts in Pcl5 fusion protein degradation within the context of proteasome function rather than independently of it. First, if the Ura3-Pcl5(1–53) processing intermediate were a Hul5 substrate, then it should be unstable when synthesized by itself; however, the truncated Ura3-Pcl5(1–53) protein synthesized by itself is completely stable even in the presence of Hul5. Second, the Ura3-Pcl5(1–53) processing product is completely stable in the *rpt2*^{RF} proteasome mutant in spite of the presence of Hul5, although other proteasomal substrates, and notably the full-length Ura3-Pcl5 protein, are only partly stabilized in the *rpt2*^{RF} mutant. If the Ura3-Pcl5(1–53) processing product were a regular proteasome substrate, dependent upon the Hul5 ubiquitin ligase for its degradation, then one would expect to see only partial stabilization of Ura3-Pcl5(1–53) in the *rpt2*^{RF} mutant and a cumulative stabilization in the *rpt2*^{RF} *hul5*Δ double mutant, contrary to what was observed. Third, GFP-Pcl5 is partially processed in both wild-type and *hul5*Δ mutant cells to a stable processing product but to different extents (~15% processing in the wild type versus ~70% in the *hul5*Δ mutant), again indicating that Hul5 plays a direct role in the processivity of proteasomal degradation.

How then does Hul5 affect the processivity of proteasomal degradation? One possibility is that it functions as an ancillary structural component of the 19S "base" subcomplex, whose role it is to unfold the substrate and thread the unfolded polypeptide into the 20S catalytic cavity. Binding of Hul5 could promote activity of the ATPases by allosteric changes. However, the fact that the Hul5 C878A mutant is unable to complement the *hul5*Δ phenotype argues for a role for Hul5 ubiquitin ligase activity in processive Ura3-Pcl5 degradation.

What is the mechanistic role of the E4 ubiquitin chain elongation activity of Hul5 in proteasome processivity? The simplest possibility is that it is required for tethering a stalled substrate to the proteasome. Conceivably, when the proteasome processively degrades a multidomain protein, including one domain carrying a degradation signal, such as Pcl5, and one hard-to-unfold domain, such as Ura3, then stalled substrate molecules of the Ura3-Pcl5(1–53) type could, with a certain frequency, escape from the proteasome. Since this molecule has lost its degradation signal, once escaped, it would be completely stable. The role of Hul5, a proteasome-associated

E4 activity, could then be to ubiquitinate the Ura3 moiety of the stalled substrate, thereby tethering it to the proteasome and enabling additional time to unfold the stable protein domain. Contradicting this simple model, however, is the observation that in the *hul5*Δ mutant, the processed product is still degraded, albeit with a half-life of about 20 min. In contrast, the directly synthesized Ura3-Pcl5(1–53) protein is completely stable. Similarly, the Ura3-Pcl5(1–53) degradation product generated in the *rpt2*^{RF} mutant also appears to be completely stable. How then can the degradation of the Ura3-Pcl5(1–53) processing product in the *hul5*Δ mutant be explained? We cannot exclude the possibility that the processing product garners a molecular modification during its residency at the proteasome, which converts it into a proteasome substrate that is still slowly degraded in the absence of *HUL5* but not in the *rpt2*^{RF} mutant. An alternative possibility is that the Ura3-Pcl5(1–53) processing product remains tethered to the proteasome in the *hul5*Δ mutant due to the continuous pulling action of the 19S ATPases until the molecule is eventually unfolded and threaded into the catalytic cavity. In the *rpt2*^{RF} mutant, since the proteasome has a weaker grip on the substrate due to reduced ATPase activity, the stalled partial degradation product could escape the proteasome and therefore be completely stabilized.

If the latter model holds true, then what is the role of Hul5's ubiquitin ligase activity if not to tether the substrate to the proteasome? Since unfolding of the tethered protein domain is one of the challenges confronting the proteasome with this type of substrate, we speculate that polyubiquitination of this domain by Hul5 may facilitate its unfolding. The presence of extended polyubiquitin chains, many times larger than the substrate, linked to different sites on the substrate structure might destabilize this structure by "entropic unfolding" (11), i.e., subjecting it to physical pulling forces due to the entropy of the attached ubiquitin chains, causing destabilization and transient unfolding of the protein structure. The transiently unfolded polypeptide could then be captured by the 19S ATPases and threaded into the proteasome.

In the other instance of accumulation of a partially degraded processing product in the *hul5*Δ mutant, fusion of the ERAD substrates CPY* and Sec61-2L to the Leu2 protein led to transient appearance of a Leu2-containing fragment in wild-type cells and to stable accumulation of this fragment in *hul5*Δ mutant cells (23). The authors' conclusion is that Hul5 contributes to the extraction of the transmembrane substrate from the ER membrane by promoting its interaction with Cdc48. Here we have shown that a cytoplasmic fusion protein substrate exhibits the same requirement for Hul5 and that processivity of that substrate's degradation is dependent on proteasomal ATPases as well. In light of our results, we suggest that the data obtained with ERAD fusion substrates (23) are also consistent with Hul5-mediated polyubiquitination promoting "entropic pulling" of the membrane protein, similar to the mechanism proposed for Hsp70 function in protein translocation (4).

It is striking that Hul5, which was formerly shown to generally promote proteasome activity (3), was found in the present study and in the work of Kohlmann et al. (23) to cause partial degradation of multidomain proteins. Of note, these last two studies used artificial fusion protein substrates, raising the question of whether this role of Hul5 also applies to natural multidomain proteins. It is possible that instances of natural multidomain proteins being processed rather than fully degraded in the *hul5*Δ mutant await discovery. It is also possible, however, that proteins inherently prone to processing, due to a combination of a highly structured domain with an adjacent "low-grip" polypeptide sequence, are selected against, because polypeptides, such as Ura3-Pcl5, that transiently but consistently "jam" the proteasome even in the wild-type background are expected to be deleterious to the cell. Therefore, the main role of Hul5 may be to help processively degrade cellular proteins that have become hard to unfold due to cross-linking or aggregation rather than to their inherent structural properties.

ACKNOWLEDGMENTS

We thank Dick Kulka, Johannes Hegemann, Bernat Crosas, and Michael Glickman for plasmids and strains, Tamar Ziv and the Smoler proteomics center for tryptic peptide analysis, Avram Hershko and Michael Glickman for helpful discussions, and Dan Finley and Sara Selig for comments on the manuscript.

This research project was supported by a grant from the Israel Science Foundation.

REFERENCES

1. **Aviram, S., E. Simon, T. Gildor, F. Glaser, and D. Kornitzer.** 2008. Autophosphorylation-induced degradation of the Pho85 cyclin Pcl5 is essential for response to amino acid limitation. Mol. Cell. Biol. **28:**6858–6869.
2. **Chernova, T. A., K. D. Allen, L. M. Wesoloski, J. R. Shanks, Y. O. Chernoff, and K. D. Wilkinson.** 2003. Pleiotropic effects of Ubp6 loss on drug sensitivities and yeast prion are due to depletion of the free ubiquitin pool. J. Biol. Chem. **278:**52102–52115.
3. **Crosas, B., J. Hanna, D. S. Kirkpatrick, D. P. Zhang, Y. Tone, N. A. Hathaway, C. Buecker, D. S. Leggett, M. Schmidt, R. W. King, S. P. Gygi, and D. Finley.** 2006. Ubiquitin chains are remodeled at the proteasome by opposing ubiquitin ligase and deubiquitinating activities. Cell **127:**1401–1413.
4. **De Los Rios, P., A. Ben-Zvi, O. Slutsky, A. Azem, and P. Goloubinoff.** 2006. Hsp70 chaperones accelerate protein translocation and the unfolding of stable protein aggregates by entropic pulling. Proc. Natl. Acad. Sci. U. S. A. **103:**6166–6171.
5. **Ellison, M. J., and M. Hochstrasser.** 1991. Epitope-tagged ubiquitin. A new probe for analyzing ubiquitin function. J. Biol. Chem. **266:**21150–21157.
6. **Finley, D.** 2009. Recognition and processing of ubiquitin-protein conjugates by the proteasome. Annu. Rev. Biochem. **78:**477–513.
7. **Gerlinger, U. M., R. Gueckel, M. Hoffmann, D. H. Wolf, and W. Hilt.** 1997. Yeast cycloheximide-resistant crl mutants are proteasome mutants defective in protein degradation. Mol. Biol. Cell **8:**2487–2499.
8. **Ghislain, M., A. Udvardy, and C. Mann.** 1993. S. cerevisiae 26S protease mutants arrest cell division in G_2/metaphase. Nature **366:**358–362.
9. **Gilon, T., O. Chomsky, and R. G. Kulka.** 1998. Degradation signals for ubiquitin system proteolysis in Saccharomyces cerevisiae. EMBO J. **17:**2759–2766.
10. **Glickman, M. H., D. M. Rubin, O. Coux, I. Wefes, G. Pfeifer, Z. Cjeka, W. Baumeister, V. A. Fried, and D. Finley.** 1998. A subcomplex of the proteasome regulatory particle required for ubiquitin-conjugate degradation and related to the COP9-signalosome and eIF3. Cell **94:**615–623.
11. **Goloubinoff, P., and P. De Los Rios.** 2007. The mechanism of Hsp70 chaperones: (entropic) pulling the models together. Trends Biochem. Sci. **32:**372–380.
12. **Groll, M., L. Ditzel, J. Lowe, D. Stock, M. Bochtler, H. D. Bartunik, and R. Huber.** 1997. Structure of 20S proteasome from yeast at 2.4 A resolution. Nature **386:**463–471.
13. **Guterman, A., and M. H. Glickman.** 2004. Complementary roles for Rpn11 and Ubp6 in deubiquitination and proteolysis by the proteasome. J. Biol. Chem. **279:**1729–1738.
14. **Hanna, J., N. A. Hathaway, Y. Tone, B. Crosas, S. Elsasser, D. S. Kirkpatrick, D. S. Leggett, S. P. Gygi, R. W. King, and D. Finley.** 2006. Deubiquitinating enzyme Ubp6 functions noncatalytically to delay proteasomal degradation. Cell **127:**99–111.
15. **Heinemeyer, W., M. Fischer, T. Krimmer, U. Stachon, and D. H. Wolf.** 1997. The active sites of the eukaryotic 20 S proteasome and their involvement in subunit precursor processing. J. Biol. Chem. **272:**25200–25209.
16. **Hershko, A., and A. Ciechanover.** 1998. The ubiquitin system. Annu. Rev. Biochem. **67:**425–479.

17. **Hope, I. A., and K. Struhl.** 1986. Functional dissection of a eukaryotic transcriptional activator protein, GCN4 of yeast. Cell **46:**885–894.
18. **Hoppe, T., K. Matuschewski, M. Rape, S. Schlenker, H. D. Ulrich, and S. Jentsch.** 2000. Activation of a membrane-bound transcription factor by regulated ubiquitin/proteasome-dependent processing. Cell **102:**577–586.
19. **Hoyt, M. A., J. Zich, J. Takeuchi, M. Zhang, C. Govaerts, and P. Coffino.** 2006. Glycine-alanine repeats impair proper substrate unfolding by the proteasome. EMBO J. **25:**1720–1729.
20. **Jackson, B. M., C. M. Drysdale, K. Natarajan, and A. G. Hinnebusch.** 1996. Identification of seven hydrophobic clusters in GCN4 making redundant contributions to transcriptional activation. Mol. Cell. Biol. **16:**5557–5571.
21. **Johnston, J. A., E. S. Johnson, P. R. Waller, and A. Varshavsky.** 1995. Methotrexate inhibits proteolysis of dihydrofolate reductase by the N-end rule pathway. J. Biol. Chem. **270:**8172–8178.
22. **Kisselev, A. F., M. Garcia-Calvo, H. S. Overkleeft, E. Peterson, M. W. Pennington, H. L. Ploegh, N. A. Thornberry, and A. L. Goldberg.** 2003. The caspase-like sites of proteasomes, their substrate specificity, new inhibitors and substrates, and allosteric interactions with the trypsin-like sites. J. Biol. Chem. **278:**35869–35877.
23. **Kohlmann, S., A. Schafer, and D. H. Wolf.** 2008. Ubiquitin ligase Hul5 is required for fragment-specific substrate degradation in endoplasmic reticulum-associated degradation. J. Biol. Chem. **283:**16374–16383.
24. **Koodathingal, P., N. E. Jaffe, D. A. Kraut, S. Prakash, S. Fishbain, C. Herman, and A. Matouschek.** 2009. ATP-dependent proteases differ substantially in their ability to unfold globular proteins. J. Biol. Chem. **284:**18674–18684.
25. **Kornitzer, D.** 2002. Monitoring protein degradation. Methods Enzymol. **351:**639–647.
26. **Kuttler, C., A. K. Nussbaum, T. P. Dick, H. G. Rammensee, H. Schild, and K. P. Hadeler.** 2000. An algorithm for the prediction of proteasomal cleavages. J. Mol. Biol. **298:**417–429.
27. **Lee, D. H., and A. L. Goldberg.** 1996. Selective inhibitors of the proteasome-dependent and vacuolar pathways of protein degradation in Saccharomyces cerevisiae. J. Biol. Chem. **271:**27280–27284.
28. **Leggett, D. S., J. Hanna, A. Borodovsky, B. Crosas, M. Schmidt, R. T. Baker, T. Walz, H. Ploegh, and D. Finley.** 2002. Multiple associated proteins regulate proteasome structure and function. Mol. Cell **10:**495–507.
29. **Martin, A., T. A. Baker, and R. T. Sauer.** 2008. Pore loops of the AAA+ ClpX machine grip substrates to drive translocation and unfolding. Nat. Struct. Mol. Biol. **15:**1147–1151.
30. **Martin, A., T. A. Baker, and R. T. Sauer.** 2008. Protein unfolding by a AAA+ protease is dependent on ATP-hydrolysis rates and substrate energy landscapes. Nat. Struct. Mol. Biol. **15:**139–145.
31. **McCusker, J. H., and J. E. Haber.** 1988. Cycloheximide-resistant temperature-sensitive lethal mutations of *Saccharomyces cerevisiae*. Genetics **119:**303–315.
32. **Meimoun, A., T. Holtzman, Z. Weissman, H. J. McBride, D. J. Stillman, G. R. Fink, and D. Kornitzer.** 2000. Degradation of the transcription factor Gcn4 requires the kinase Pho85 and the SCF(CDC4) ubiquitin-ligase complex. Mol. Biol. Cell **11:**915–927.
33. **Nussbaum, A. K., T. P. Dick, W. Keilholz, M. Schirle, S. Stevanovic, K. Dietz, W. Heinemeyer, M. Groll, D. H. Wolf, R. Huber, H. G. Rammensee, and H. Schild.** 1998. Cleavage motifs of the yeast 20S proteasome beta subunits deduced from digests of enolase 1. Proc. Natl. Acad. Sci. U. S. A. **95:**12504–12509.
34. **Orian, A., A. L. Schwartz, A. Israel, S. Whiteside, C. Kahana, and A. Ciechanover.** 1999. Structural motifs involved in ubiquitin-mediated processing of the NF-kappaB precursor p105: roles of the glycine-rich region and a downstream ubiquitination domain. Mol. Cell. Biol. **19:**3664–3673.
35. **Palombella, V. J., O. J. Rando, A. L. Goldberg, and T. Maniatis.** 1994. The ubiquitin-proteasome pathway is required for processing the Nf-kappaB1 precursor protein and the activation of Nf-kappaB. Cell **78:**773–785.
36. **Pickart, C. M., and R. E. Cohen.** 2004. Proteasomes and their kin: proteases in the machine age. Nat. Rev. Mol. Cell Biol. **5:**177–187.
37. **Piwko, W., and S. Jentsch.** 2006. Proteasome-mediated protein processing by bidirectional degradation initiated from an internal site. Nat. Struct. Mol. Biol. **13:**691–697.
38. **Prakash, S., L. Tian, K. S. Ratliff, R. E. Lehotzky, and A. Matouschek.** 2004. An unstructured initiation site is required for efficient proteasome-mediated degradation. Nat. Struct. Mol. Biol. **11:**830–837.
39. **Rock, K. L., C. Gramm, L. Rothstein, K. Clark, R. Stein, L. Dick, D. Hwang, and A. L. Goldberg.** 1994. Inhibitors of the proteasome block the degradation of most cell proteins and the generation of peptides presented on MHC class I molecules. Cell **78:**761–771.
40. **Rubin, D. M., M. H. Glickman, C. N. Larsen, S. Dhruvakumar, and D. Finley.** 1998. Active site mutants in the six regulatory particle ATPases reveal multiple roles for ATP in the proteasome. EMBO J. **17:**4909–4919.
41. **Sauer, R. T., D. N. Bolon, B. M. Burton, R. E. Burton, J. M. Flynn, R. A. Grant, G. L. Hersch, S. A. Joshi, J. A. Kenniston, I. Levchenko, S. B. Neher, E. S. Oakes, S. M. Siddiqui, D. A. Wah, and T. A. Baker.** 2004. Sculpting the proteome with AAA(+) proteases and disassembly machines. Cell **119:**9–18.
42. **Schrader, E. K., K. G. Harstad, and A. Matouschek.** 2009. Targeting proteins for degradation. Nat. Chem. Biol. **5:**815–822.
43. **Shemer, R., A. Meimoun, T. Holtzman, and D. Kornitzer.** 2002. Regulation of the transcription factor Gcn4 by Pho85 cyclin PCL5. Mol. Cell. Biol. **22:**5395–5404.
44. **Smith, D. M., G. Kafri, Y. Cheng, D. Ng, T. Walz, and A. L. Goldberg.** 2005. ATP binding to PAN or the 26S ATPases causes association with the 20S proteasome, gate opening, and translocation of unfolded proteins. Mol. Cell **20:**687–698.
45. **Tian, L., R. A. Holmgren, and A. Matouschek.** 2005. A conserved processing mechanism regulates the activity of transcription factors Cubitus interruptus and NF-kappaB. Nat. Struct. Mol. Biol. **12:**1045–1053.
46. **Verma, R., L. Aravind, R. Oania, W. H. McDonald, J. R. Yates III, E. V. Koonin, and R. J. Deshaies.** 2002. Role of Rpn11 metalloprotease in deubiquitination and degradation by the 26S proteasome. Science **298:**611–615.
47. **Verma, R., S. Chen, R. Feldman, D. Schieltz, J. Yates, J. Dohmen, and R. J. Deshaies.** 2000. Proteasomal proteomics: identification of nucleotide-sensitive proteasome-interacting proteins by mass spectrometric analysis of affinity-purified proteasomes. Mol. Biol. Cell **11:**3425–3439.
48. **Wilk, S., and M. Orlowski.** 1983. Evidence that pituitary cation-sensitive neutral endopeptidase is a multicatalytic protease complex. J. Neurochem. **40:**842–849.
49. **You, J., and C. M. Pickart.** 2001. A HECT domain E3 enzyme assembles novel polyubiquitin chains. J. Biol. Chem. **276:**19871–19878.
50. **Zhang, F., Z. Wu, P. Zhang, G. Tian, D. Finley, and Y. Shi.** 2009. Mechanism of substrate unfolding and translocation by the regulatory particle of the proteasome from Methanocaldococcus jannaschii. Mol. Cell **34:**485–496.
51. **Zhang, M., and P. Coffino.** 2004. Repeat sequence of Epstein-Barr virus-encoded nuclear antigen 1 protein interrupts proteasome substrate processing. J. Biol. Chem. **279:**8635–8641.